

Spatial anisotropy of the acousto-optical efficiency in lithium niobate crystals

A. S. Andrushchak,¹ E. M. Chernyivsky,¹ Z. Yu. Gotra,^{1,2} M. V. Kaidan,¹ A. V. Kityk,^{3,a)}
 N. A. Andrushchak,¹ T. A. Maksymyuk,¹ B. G. Mytsyk,⁴ and W. Schranz⁵

¹Lviv Polytechnic National University, 12 S. Bandery Str., 79013 Lviv, Ukraine

²Rzeszow Technical University, ul. W. Pola 2, PL-35959 Rzeszow, Poland

³Faculty of Electrical Engineering, Czestochowa University of Technology, Al. Armii Krajowej 17, PL-42200 Czestochowa, Poland

⁴Karpenko Physico-Mechanical Institute, 5 Naukova Str., 79601 Lviv, Ukraine

⁵Faculty of Physics, University of Vienna, Boltzmannngasse 5, A-1090 Vienna, Austria

(Received 6 June 2010; accepted 3 October 2010; published online 30 November 2010)

We report the spatial anisotropy of the acousto-optic (AO) figure of merit M_2 in LiNbO₃ crystals. The analysis is based on the indicative surfaces being calculated for several geometries of the AO diffraction. Basing on these results the most efficient geometries of AO cells made of LiNbO₃ crystals are determined. It is revealed that the cells made of certain nondirect crystal cuts provide several times better AO diffraction efficiency comparing to the traditional ones, i.e., made of direct cuts of LiNbO₃. The obtained results present considerable practical interest since may be useful in a designing of highly efficient AO cells made of LiNbO₃ crystals. The methodology developed in the present work may be applied to other crystal materials as well. © 2010 American Institute of Physics. [doi:10.1063/1.3510518]

I. INTRODUCTION

The characteristics of the acousto-optic (AO) cells made of crystal materials are defined much by the geometry of the AO interaction occurring in the anisotropic media. Its proper choice provides the best diffraction efficiency, and accordingly, minimizes an operating power of the AO cells which constitute the key elements of many optoelectronic devices. While such cells are being designed the knowledge on the spatial anisotropy of the figure of merit (FM) $M_2(\varphi, \theta)$ is strongly required. It allows not only to predict the basic characteristics of the AO device but also to optimize the cell geometry.¹⁻⁷ Actual work deals with the lithium niobate (LiNbO₃) crystals being known due to their broad range of applications, namely as highly efficient electro-optic,⁸⁻¹⁰ nonlinear optic,^{8,11-13} photorefractive,^{8,14} or acousto-optical^{5,8,15,16} material. However, even up to date these crystals, likewise as many other anisotropic materials, are not always used in the most optimized geometries. In regards to the electro-optical effect this problem was recently discussed in details, see Refs. 4 and 9. It was revealed, for example, that the cell made of the X₁/54°—cuts of LiNbO₃ provides of about three times higher modulation efficiency compared to the ones made in their traditional geometry, i.e., as rectangular slabs being cut perpendicularly to the principal crystallographic axes. Similar examples may be given also concerning other properties of these crystals like, e.g., the piezooptic and/or photoelastic effects.¹⁷⁻¹⁹ In the present paper we hence extend the spatial anisotropy analysis on the AO properties of LiNbO₃ crystals having in goal to determine the most optimal geometry of the AO coupling. Our search is based on the indicative surfaces (ISs) technique.^{17,20-23} Re-

quired for such analysis the optical refraction indices, photoelastic and elastic tensor constants of LiNbO₃ are available in our recently published work.²⁴ For this reason current consideration will be limited mainly by a derivation of basic equations, calculations of the ISs that describe the spatial anisotropy of the FM $M_2(\varphi, \theta)$ and their analysis.

II. BASIC RELATIONSHIPS

To obtain the IS of the FM $M_2(\varphi, \theta)$ one must determine first the vector characteristics of the interacting waves that define the effective photoelastic constant p_{ef} via the relation:^{6,7}

$$p_{ef} = \mathbf{i}_\mu \mathbf{i}_\nu \hat{p} \mathbf{a} \mathbf{f}_q, \quad (1)$$

where $\mu, \nu = 1, 2$; $q = 1, 2, 3$; \mathbf{i}_μ and \mathbf{i}_ν are the polarization unit vectors of the incident and diffracted optical waves, respectively, \mathbf{f}_q is the polarization unit vector of the acoustic wave, \mathbf{a} is the unit vector parallel to the direction of acoustic wave propagation, \hat{p} is the photoelastic tensor given in the principal crystallophysical axes set. In the case when $\mu = \nu$ the isotropic diffraction is considered, otherwise ($\mu \neq \nu$) one deals with anisotropic diffraction. According to⁶ the subscript index q defines one of three possible acoustic wave polarizations corresponding either to the slow ($q = 1$) or fast ($q = 2$) transverse (shear) acoustic waves or to the longitudinal ($q = 3$) acoustic wave. Here Eq. (1) likewise the description following below are given in the coordinateless form. The light polarization vectors $\mathbf{i}_\mu, \mathbf{i}_\nu$ can be found by solving the Maxwell's equations for the plane electromagnetic wave propagating in the anisotropic media. Assuming that $\mathbf{i}_\omega \mathbf{k} = 0$ one obtains:⁶

$$\hat{\gamma} \mathbf{i}_\omega - \mathbf{k}(\mathbf{k} \hat{\gamma} \mathbf{i}_\omega) = n_\omega^{-2} \mathbf{i}_\omega, \quad (2)$$

^{a)}Electronic mail: kityk@ap.univie.ac.at.

where the subscript index ω coincides with μ or ν , \mathbf{k} is the unit vector parallel to the propagation direction of the light; $\hat{\eta}$ is the dielectric permittivity given in the principal crystallophysical axes set, n_ω is the optical refraction index defined as:⁶

$$n_\omega = (\mathbf{i}_\omega \hat{\eta} \mathbf{i}_\omega)^{-1/2}. \quad (3)$$

Equation (2) should be solved separately for the incident and diffracted beams taking into account that the scalar product $\mathbf{i}_\mu \mathbf{i}_\nu = \delta_{\mu\nu}$, where $\delta_{\mu\nu}$ is the Kronecker delta. The vector characteristics of the elastic waves can be found by solving the Christoffel's elastodynamics wave equation. Taking into account that $\mathbf{f}_q \mathbf{f}_{q'} = \delta_{qq'}$ it then reads as:⁶

$$\mathbf{a} \hat{\mathbf{c}} \mathbf{a} \mathbf{f} = \rho V_q^2 \mathbf{f}_q, \quad (4)$$

where ρ is the crystal density, V_q is the velocity of the acoustic wave, $\hat{\mathbf{c}}$ is the elastic tensor given in the principal axes set. The relationship between the interacting optical and acoustical waves is defined via the diffraction angle θ^* as follows:^{1,6}

$$\mathbf{k} \mathbf{a} = \cos(90^\circ - \theta^*) = \sin \theta^*, \quad (5)$$

It is commonly accepted that the basic AO characteristics of the crystals materials are presented by means of several FM coefficients²⁵ among of which the most important is the FM coefficient M_2 characterizing the diffraction efficiency of the AO media. It reads as:²⁶

$$M_2 = \frac{n_\mu^3 n_\nu^3 p_{ef}^2}{\rho V_q^3} \cos \beta_\mu \cos \beta_\nu \cos \gamma_a, \quad (6)$$

where β_μ and β_ν are the shift angles between the wave-fronts and propagation directions for the incident and diffracted light given by the following equation:⁶

$$\text{tg} \beta_\omega = n_\omega^{-2} (\mathbf{k} \hat{\eta} \mathbf{i}_\omega), \quad (7)$$

whereas γ_a is the shift angle between the wave-front and propagation direction for the acoustic wave being defined as:

$$\cos \gamma_a = \rho V_q^2 (\mathbf{a} (\hat{\mathbf{c}} \mathbf{f}) (\hat{\mathbf{c}} \mathbf{f}) \mathbf{a})^{-1/2}. \quad (8)$$

One should be emphasized that the angels β_μ and β_ν are small thus to a good approximation $\cos \beta_\mu$ and $\cos \beta_\nu$ in Eq. (6) may be simply set to 1. Similar remark is not valid in regard to the angle γ_a , which may be quite large and must be considered explicitly.

III. EQUATIONS OF THE ISS $p_{ef}(\varphi, \theta)$ and $M_2(\varphi, \theta)$

Spatial analysis of the AO characteristics may be largely simplified by considering, like, e.g., in Refs. 1, 6, and 27, the particular case when the propagation directions of the optical and acoustical waves are perpendicular each other ($\mathbf{k} \perp \mathbf{a}$) thus the diffraction angle θ^* in Eq. (5) is equal 90° . By doing so the wavelengths of the optical (λ) and acoustical (Λ) waves appears to be omitted from the consideration what reduces the number of dependent parameters. In the following we apply the methodology developed in our previous works (see, e.g., Refs. 4 and 17–23) for the electro-optic and piezo-optic effects in crystalline materials which is based on

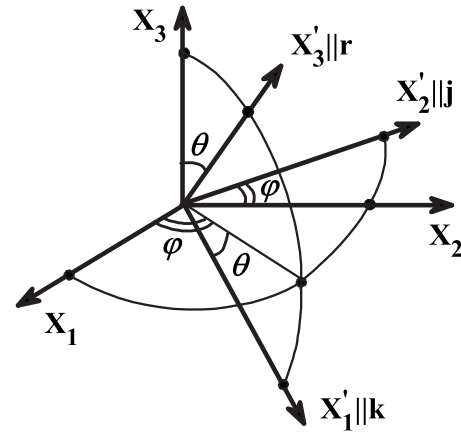


FIG. 1. Spatial position of the rotating coordinate system X'_1, X'_2, X'_3 with respect to the crystallophysical axes set X_1, X_2, X_3 for the uniaxial crystals. The axes X'_1, X'_2, X'_3 coincide with the propagation direction \mathbf{k} of the light and its two possible polarizations ($\mathbf{j} \parallel \mathbf{i}_\omega$ or $\mathbf{r} \parallel \mathbf{i}_\omega$) such that $\mathbf{k} \parallel X'_1, \mathbf{j} \parallel X'_2, \mathbf{r} \parallel X'_3$.

the analysis of the IS. The directional cosines for the radius vector \mathbf{r} (see Fig. 1) are defined in the crystallophysical axes set X_1, X_2, X_3 as:^{4,20,21}

$$\alpha_{r1} = \sin \theta \cos \varphi, \quad \alpha_{r2} = \sin \theta \sin \varphi, \quad \alpha_{r3} = \cos \theta, \quad (9)$$

whereas the rotating axis set X'_1, X'_2, X'_3 coincides, as usual, with the propagation direction \mathbf{k} of the light and its two possible polarizations $\mathbf{j} \parallel \mathbf{i}_\omega$ and $\mathbf{r} \parallel \mathbf{i}_\omega$ such that $\mathbf{k} \parallel X'_1, \mathbf{j} \parallel X'_2$, and $\mathbf{r} \parallel X'_3$. Thinking of optically uniaxial crystals, to which LiNbO₃ belongs, the directional cosines of the unit vectors \mathbf{j} and \mathbf{k} (see Fig. 1) may be expressed via the angles θ and φ as:^{4,20,21}

$$\alpha_{j1} = -\sin \varphi, \quad \alpha_{j2} = \cos \varphi, \quad \alpha_{j3} = 0; \quad (10)$$

$$\alpha_{k1} = \cos \theta \cos \varphi, \quad \alpha_{k2} = \cos \theta \sin \varphi, \quad \alpha_{k3} = -\sin \theta. \quad (11)$$

Here \mathbf{j} or \mathbf{r} coincides with the polarization of the ordinary or extraordinary optical waves, respectively. Accordingly, $\mathbf{k} \perp \mathbf{a}$ and $\mathbf{k} \perp \mathbf{i}_\omega$ thus likewise to other types of the optical parametric effects considered, e.g., in Refs. 4 and 17–23, one may build up three commonly used types of ISs for a given acoustic wave polarization ($q=1, 2$, or 3) separately for isotropic and anisotropic diffractions, namely so-called:

- Longitudinal IS ($\mathbf{i}_\mu \parallel \mathbf{a} \parallel \mathbf{r}$);
- Transverse optical IS ($\mathbf{i}_\mu \parallel \mathbf{r}, \mathbf{a} \parallel \mathbf{j}$);
- Transverse acoustic IS ($\mathbf{a} \parallel \mathbf{r}, \mathbf{i}_\mu \parallel \mathbf{j}$).

Table I presents a complete set of corresponding equations describing the ISs of the effective photoelastic constant $p_{ef}(\varphi, \theta)$ as well as the IS of the FM $M_2(\varphi, \theta)$ for different types of the AO diffraction as specified in the left column of this table. The subscript index in the brackets specifies the diffraction type, i.e., the isotropic (is) or anisotropic (as) one. The superscript index in the brackets specifies the type of the IS for which either vector \mathbf{i}_μ , vector \mathbf{a} or both they coincide(s) with the radius vector \mathbf{r} ; this is also mentioned in the second column from the left of Table I. The refractive indices n_r and n_j as well as the angels β_r and β_j are defined by Eqs. (3) and (7) taking into account that $\mathbf{r} \parallel \mathbf{i}_\omega$ or $\mathbf{j} \parallel \mathbf{i}_\omega$, correspond-

TABLE I. Basic equations describing the ISs of the effective photoelastic constant $p_{\text{ef}}(\varphi, \theta)$ and the ISs of the FM $M_2(\varphi, \theta)$ for different types of the AO diffraction. The subscript index in the brackets specifies the diffraction type, isotropic (is) or anisotropic (as). The superscript index in the brackets specifies the type of the IS, i.e., which of the vectors \mathbf{i}_μ , \mathbf{a} or both they coincide(s) with the radius vector \mathbf{r} as given in the second column from the left.

Diffraction type	Vector set	Equations of the IS	
		Effective photoelastic constant p_{ef}	FM M_2
Isotropic	$\mathbf{i}_\mu \parallel \mathbf{a} \parallel \mathbf{r}$	$p_{\text{ef(is)}}^{(i,a)} = \mathbf{r} \hat{\rho} \mathbf{r} \mathbf{f}_q$	$M_{2(\text{is})}^{(i,a)} = \frac{n_r^6 (p_{\text{ef(is)}}^{(i,a)})^2}{\rho V_r^3} \cos^2 \beta_r \cos \gamma_r$ (12)
Isotropic	$\mathbf{i}_\mu \parallel \mathbf{r}, \mathbf{a} \parallel \mathbf{j}, \mathbf{i}_\mu \perp \mathbf{a}$	$p_{\text{ef(is)}}^{(i)} = \mathbf{r} \hat{\rho} \mathbf{j} \mathbf{f}_q$	$M_{2(\text{is})}^{(i)} = \frac{n_r^6 (p_{\text{ef(is)}}^{(i)})^2}{\rho V_j^3} \cos^2 \beta_r \cos \gamma_j$ (13)
Isotropic	$\mathbf{a} \parallel \mathbf{r}, \mathbf{i}_\mu \parallel \mathbf{j}, \mathbf{i}_\mu \perp \mathbf{a}$	$p_{\text{ef(is)}}^{(a)} = \mathbf{j} \hat{\rho} \mathbf{r} \mathbf{f}_q$	$M_{2(\text{is})}^{(a)} = \frac{n_j^6 (p_{\text{ef(is)}}^{(a)})^2}{\rho V_r^3} \cos^2 \beta_j \cos \gamma_r$ (14)
Anisotropic	$\mathbf{i}_\mu \parallel \mathbf{a} \parallel \mathbf{r}, \mathbf{i}_\nu \parallel \mathbf{j}$	$p_{\text{ef(as)}}^{(i,a)} = \mathbf{r} \hat{\rho} \mathbf{r} \mathbf{f}_q$	$M_{2(\text{as})}^{(i,a)} = \frac{n_r^3 n_j^3 (p_{\text{ef(as)}}^{(i,a)})^2}{\rho V_r^3} \cos \beta_r \cos \beta_j \cos \gamma_r$ (15)
Anisotropic	$\mathbf{i}_\mu \parallel \mathbf{r}, \mathbf{i}_\nu \parallel \mathbf{a} \parallel \mathbf{j}, \mathbf{i}_\mu \perp \mathbf{a}$	$p_{\text{ef(as)}}^{(i)} = \mathbf{r} \hat{\rho} \mathbf{j} \mathbf{f}_q$	$M_{2(\text{as})}^{(i)} = \frac{n_r^3 n_j^3 (p_{\text{ef(as)}}^{(i)})^2}{\rho V_j^3} \cos \beta_r \cos \beta_j \cos \gamma_j$ (16)
Anisotropic	$\mathbf{i}_\nu \parallel \mathbf{a} \parallel \mathbf{r}, \mathbf{i}_\mu \parallel \mathbf{j}, \mathbf{i}_\mu \perp \mathbf{a}$	$p_{\text{ef(as)}}^{(a)} = \mathbf{j} \hat{\rho} \mathbf{r} \mathbf{f}_q$	$M_{2(\text{as})}^{(a)} = \frac{n_r^3 n_j^3 (p_{\text{ef(as)}}^{(a)})^2}{\rho V_r^3} \cos \beta_r \cos \beta_j \cos \gamma_r$ (17)

ingly. Similarly, the elastic wave velocities V_r or V_j as well as the shift angles γ_r or γ_j can be determined by means of Eqs. (4) and (8) if $\mathbf{r} \parallel \mathbf{a}$ or $\mathbf{j} \parallel \mathbf{a}$, respectively. One must notice that the photoelastic constant is symmetric with respect to the first two indices. For this reason Eqs. (15) and (17) coincide each other which reduces the number of ISs to five, i.e., for each acoustic wave polarization ($q=1, 2$, or 3).

IV. SPATIAL ANALYSIS OF THE IS $M_2(\varphi, \theta)$ IN LiNbO_3 CRYSTAL

To calculate the ISs of the FM $M_2(\varphi, \theta)$ in LiNbO_3 crystal we substituted into Eq. (12)–(17) the crystal density $\rho = 4628 \text{ kg/m}^3$, ordinary (n_o) and extraordinary (n_e) refractive indices likewise the magnitudes of the elastic (C_{ij}) and photoelastic (p_{ij}) tensor constants as determined in Ref. 24: $n_o = 2.2865$, $n_e = 2.2034$, $C_{11} = 199.2 \text{ GPa}$, $C_{12} = 54.7 \text{ GPa}$, $C_{13} = 70.0 \text{ GPa}$, $C_{14} = 7.9 \text{ GPa}$, $C_{33} = 240 \text{ GPa}$, $C_{44} = 59.9 \text{ GPa}$, $p_{11} = -0.021$, $p_{12} = 0.060$, $p_{13} = 0.172$, $p_{31} = 0.141$, $p_{33} = 0.118$, $p_{14} = -0.052$, $p_{41} = -0.109$, $p_{44} = 0.121$. The extreme magnitudes on the $M_2(\varphi, \theta)$ surfaces have been found numerically and are presented in Table II. The geometries characterizing by a strong AO coupling are marked by bold font for the regimes of both isotropic and anisotropic AO diffractions on the transverse ($q=1, 2$) or longitudinal ($q=3$) acoustical waves, respectively. In such a way we indeed have determined the geometry of the AO cells which are expected to provide the best diffraction efficiency for each particular type of the AO diffraction. Explicitly for these geometries we present the basic AO characteristics (see Table III) likewise the three-dimensional plots of corresponding ISs as well as their stereographic projections (see Fig. 2). The maximum FM with the magnitude $M_2 = 15.9 \times 10^{-15} \text{ s}^3/\text{kg}$ takes place for the anisotropic AO diffraction on shear waves ($q=1$) characterizing by the vector set $\mathbf{i}_\mu \parallel \mathbf{a} \parallel \mathbf{r}$ and $\mathbf{i}_\nu \parallel \mathbf{j}$. Such AO diffraction is indeed realized in

the cells made of nondirect $X_1/-23.3^\circ$ crystal cuts. In the case of the isotropic AO diffraction the maximum FM ($M_2 = 6.9 \times 10^{-15} \text{ s}^3/\text{kg}$) exhibits the geometry defining by the vector set $\mathbf{i}_\mu \parallel \mathbf{a} \parallel \mathbf{r}$ which in fact corresponds to the light diffraction on the shear elastic wave ($q=2$). Its magnitude only slightly exceeds the diffraction efficiency ($M_2 = 6.4 \times 10^{-15} \text{ s}^3/\text{kg}$) for the isotropic AO diffraction on the longitudinal elastic wave ($q=3$) defining by the same vector set, i.e., $\mathbf{i}_\mu \parallel \mathbf{a} \parallel \mathbf{r}$, and provided by the cells made of nondirect $X_1/46.8^\circ$ crystal cut of LiNbO_3 .

The obtained ISs $M_2(\varphi, \theta)$ [see Figs. 2(a)–2(d)] can be easily verified along the principal crystallographic directions. Table IV lists several such geometries. While the wavevectors and the polarizations of the light and acoustic waves coincide with the principal crystallographic directions the Eqs. (12)–(15) appears to be essentially reduced to the form: $M_2 = n^6 p_{\text{ef}}^2 / (\rho V^3)$ with p_{ef} being equal to just one of the photoelastic tensor component p_{ij} . For some geometries the photoelastic tensor components, like p_{35} , p_{15} , or p_{62} are equal 0 (see first, second and last row of the Table IV) which is

TABLE II. The extreme magnitudes $M_2^{(\text{ext})}$ on the ISs $M_2(\varphi, \theta)$ of LiNbO_3 crystals. The geometries characterizing by a strong AO coupling are marked by bold font for each particular type of the AO diffraction on the transverse ($q=1, 2$) or longitudinal ($q=3$) acoustic waves.

Diffraction type	Vector set	LiNbO ₃		
		$M_2^{(\text{ext})} (10^{-15} \text{ s}^3/\text{kg})$		
		$q=1$	$q=2$	$q=3$
Isotropic	$\mathbf{i}_\mu \parallel \mathbf{a} \parallel \mathbf{r}$	4.7	6.9	6.4
Isotropic	$\mathbf{i}_\mu \parallel \mathbf{r}, \mathbf{a} \parallel \mathbf{j}$	5.3	1.6	4.4
Isotropic	$\mathbf{a} \parallel \mathbf{r}, \mathbf{i}_\mu \parallel \mathbf{j}$	2.8	2.5	2.9
Anisotropic	$\mathbf{i}_\mu \parallel \mathbf{a} \parallel \mathbf{r}, \mathbf{i}_\nu \parallel \mathbf{j}$	15.9	8.6	0.5
Anisotropic	$\mathbf{i}_\mu \parallel \mathbf{r}, \mathbf{i}_\nu \parallel \mathbf{a} \parallel \mathbf{j}$	2.0	6.7	1.3

TABLE III. Basic AO characteristics of LiNbO₃ crystals for several most efficient cell geometries as marked in Table II.

IS	Acoustic polarization	Optic wave				Acoustic wave				V_q (m/s)	p_{ef}	M_2 (10^{-15} s ³ /kg)
		\mathbf{i}_μ (deg)	\mathbf{i}_ν (deg)	\mathbf{a} (deg)	\mathbf{f} (deg)	φ_a	θ_a	φ_f	θ_f			
$M_{2(is)}^{(i,a)}$	$q=2$	7	60	7	60	7	60	235	49.2	4340	0.139	6.9
$M_{2(is)}^{(i,a)}$	$q=3$	90	46.8	90	46.8	90	46.8	90	43.7	7360	0.303	6.4
$M_{2(as)}^{(i,a)}$	$q=1$	-90	23.3	0	90	-90	23.3	0	90	3480	0.154	15.9
$M_{2(as)}^{(i)}$	$q=3$...	0	90	90	90	90	90	83.2	6820	0.123	1.3

defined by the symmetry principle. Accordingly, along these directions the acousto-optical efficiency is characterized by zero magnitude in well agreement with calculated ISs $M_2(\varphi, \theta)$, see Fig. 2. The analysis of the IS and their stereographic projections also reveals that all the surfaces appear to be consistent with Curie–Neumann principle.²⁸ Clearly, the IS are invariant here with respect to the symmetry operations of the point group $3m$ describing the symmetry of the crystal structure of LiNbO₃ crystals. On the other hand, the ISs do not exhibit a totally rotational symmetry (with the axis of order infinity) what appears to be also consistent with the German's theorem.²⁹

V. CONCLUSIONS

Taken together, we have evaluated the diffraction efficiency in LiNbO₃ crystals for the cases of the isotropic and

anisotropic AO diffractions. Its spatial anisotropy has been analyzed in the terms of the ISs and their stereographic projections. The maximum diffraction efficiency with the magnitude of the FM $M_2=15.9 \times 10^{-15}$ s³/kg reveals the anisotropic AO diffraction on the shear elastic waves provided by the cells made of nondirect X₁/-23.3° crystal cut. In the case of the isotropic diffraction the maximum FM ($M_2=6.9 \times 10^{-15}$ s³/kg) exhibits the AO diffraction on the shear elastic waves in the cells also made of nondirect cut of LiNbO₃. Its magnitude is comparable with the diffraction efficiency of the isotropic AO diffraction ($M_2=6.4 \times 10^{-15}$ s³/kg) on the longitudinal elastic waves being provided by the cells made of nondirect X₁/46.8° crystal cuts. For the geometries mentioned above the diffraction efficiency exceeds nearly twice the AO efficiency of the frequently used cells that are made of the direct cuts of LiNbO₃. For comparison, the FM in this

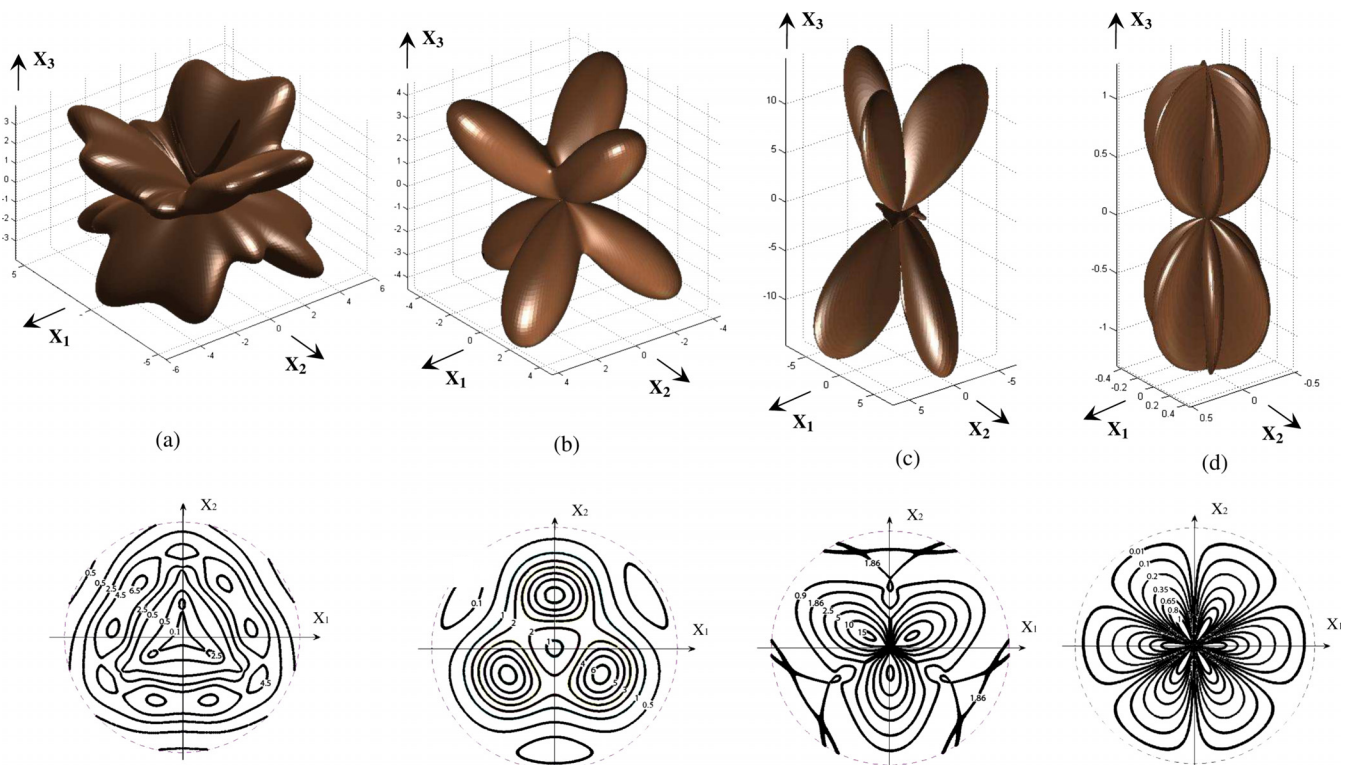


FIG. 2. (Color online) The calculated ISs of the AO FM $M_2(\varphi, \theta)$ and their stereographic projections for LiNbO₃ crystals. (a) The isotropic AO diffraction on the shear ($q=2$) elastic waves, $\mathbf{i}_\mu \parallel \mathbf{a} \parallel \mathbf{r}$; (b) the isotropic AO diffraction on the longitudinal ($q=3$) elastic waves, $\mathbf{i}_\mu \parallel \mathbf{a} \parallel \mathbf{r}$; (c) the anisotropic AO diffraction on the shear ($q=1$) elastic waves, $\mathbf{i}_\mu \parallel \mathbf{a} \parallel \mathbf{r}$, $\mathbf{i}_\nu \parallel \mathbf{j}$; (d) the anisotropic AO diffraction on the longitudinal ($q=3$) elastic waves, $\mathbf{i}_\mu \parallel \mathbf{r}$, $\mathbf{i}_\nu \parallel \mathbf{a} \parallel \mathbf{j}$. All the numbers are given in the units of 10^{-15} s³/kg.

TABLE IV. Verification of the obtained ISs $M_2(\varphi, \theta)$ [see Figs. 2(a)–2(d)] along several chosen principal crystallographic directions. While the wavevectors and polarizations of the light and acoustic waves coincides with principal crystallographic directions the Eqs. (12)–(15) appears to be essentially reduced with p_{ef} being equal to just one of the photoelastic tensor component p_{ij} .

IS, figure	Selected direction of IS (axis)	Acoustic polarization	Optic wave				Acoustic wave				p_{ef}	M_2 (10^{-15} s ³ /kg)
			\mathbf{i}_μ (deg)		\mathbf{i}_ν (deg)		\mathbf{a} (deg)		\mathbf{f} (deg)			
			φ_μ	θ_μ	φ_ν	θ_ν	φ_a	θ_a	φ_f	θ_f		
$M_{2(\text{is})}^{(i,a)}$, Fig. 2(a)	X_3	$q=2$...	0	...	0	...	0	0	90	$p_{35}=0$	0
$M_{2(\text{is})}^{(i,a)}$, Fig. 2(a)	X_1	$q=2$	0	90	0	90	0	90	...	0	$p_{15}=0$	0
$M_{2(\text{is})}^{(i,a)}$, Fig. 2(b)	X_3	$q=3$...	0	...	0	...	0	...	0	$p_{33}=0.118$	0.86
$M_{2(\text{is})}^{(i,a)}$, Fig. 2(b)	X_1	$q=3$	0	90	0	90	0	90	0	90	$p_{11}=-0.021$	0.048
$M_{2(\text{as})}^{(i,a)}$, Fig. 2(c)	X_3	$q=1$...	0	90	90	...	0	90	90	$p_{44}=0.121$	8.6
$M_{2(\text{as})}^{(i,a)}$, Fig. 2(c)	X_1	$q=1$	0	90	90	90	0	90	90	90	$p_{66}=-0.041$	0.90
$M_{2(\text{as})}^{(i)}$, Fig. 2(d)	X_3	$q=3$...	0	90	90	90	90	90	83.2	$p_{42}=0.109$	1.04
$M_{2(\text{as})}^{(i)}$, Fig. 2(d)	X_1	$q=3$	0	90	90	90	90	90	90	83.2	$p_{62}=0$	0

case is characterized by a considerably smaller magnitude of M_2 , just 2.92×10^{-15} s³/kg.⁶ The obtained results present thus a considerable practical interest since may be useful in a designing of highly efficient AO cells made of LiNbO₃ crystals. The methodology developed in the present work may be applied to other crystal materials as well. In this case the equations should be derived for each particular symmetry following the route as described in Secs. II and III.

ACKNOWLEDGMENTS

This work has been supported by STCU program (Project No. 4584) and by the Program of the Ukrainian-Polish Scientific-Technical Cooperation in years 2009–2010 [Project title: “Investigations of new crystalline materials for optoelectronics applications: characterization, geometry optimization, and improvement of their efficiency in practical applications” Project No. M/138-2009 (according to Ukrainian classification); Project No. 16 (according to Polish classification)].

¹V. S. Bondarenko, O. A. Byshevskii, N. V. Perelomova, and L. E. Chirkov, *Sov. Phys. Crystallogr.* **31**, 196 (1986).

²V. S. Bondarenko, V. P. Zorenko, and V. V. Chkalova, *Acoustooptical Modulators of Light* (Radio i Svyaz, Moscow, 1988) (in Russian).

³M. Jazbinšek and M. Zgonik, *Appl. Phys. B: Lasers Opt.* **74**, 407 (2002).

⁴A. S. Andrushchak, B. G. Mytsyk, N. M. Demyanyshyn, M. V. Kaidan, O. V. Yurkevych, S. S. Dumych, A. V. Kityk, and W. Schranz, *Opt. Lasers Eng.* **47**, 24 (2009).

⁵A. S. Andrushchak, B. G. Mytsyk, N. M. Demyanyshyn, M. V. Kaidan, and O. V. Yurkevych, Proceedings of Ninth International Conference on LFNM 2008, Alushta, Crimea, Ukraine, 2–4 October 2008, p. 66.

⁶V. I. Balakshy, V. N. Parygin, and L. E. Chirkov, *Basic Physics of Acousto-optics* (Izd. Radio i Svyaz, Moscow, 1985) (in Russian).

⁷A. Korpel, *Acousto-Optics* (Marcel Dekker, New York, 1996).

⁸Yu. S. Kuzminov, *Electro-optical and Nonlinear Optical Lithium Niobate Crystal* (Science, Moscow, 1987) (in Russian).

⁹A. S. Andrushchak, B. G. Mytsyk, N. M. Demyanyshyn, M. V. Kaidan, O. V. Yurkevych, I. M. Solskii, A. V. Kityk, and W. Schranz, *Opt. Lasers Eng.* **47**, 31 (2009).

¹⁰T.-Hs. Lee, P.-I. Wu, and C.-T. Lee, *Microw. Opt. Technol. Lett.* **49**, 2312 (2007).

¹¹E. Cantelar, M. Domenech, G. Lifante, F. Cusso, A. C. Busacca, S. Riva-Sanseverino, A. Parisi, and A. C. Cino, *Electron. Lett.* **43**, 632 (2007).

¹²Y. Kong, S. Liu, Y. Zhao, H. Liu, S. Chen, and J. Xu, *Appl. Phys. Lett.* **91**, 081908 (2007).

¹³D. Djukic, G. Cerda-Pons, R. M. Roth, R. M. Osgood, Jr., S. Bakhru, and H. Bakhru, *Appl. Phys. Lett.* **90**, 171116 (2007).

¹⁴D. R. Evans and G. Cook, *J. Nonlinear Opt. Phys. Mater.* **16**, 271 (2007).

¹⁵R. Rimeika, D. Čiplys, and P. Každašis, *Appl. Phys. Lett.* **90**, 181935 (2007).

¹⁶A. S. Andrushchak, B. G. Mytsyk, I. M. Solskii, M. V. Kaidan, T. I. Voronyak, N. M. Demyanyshyn, and O. V. Yurkevych, Proceedings of International Conference on TCSET'2008, Lviv-Slavske, Ukraine, 19–23 February 2008, p. 392.

¹⁷B. G. Mytsyk, Y. V. Pryriz, and A. S. Andrushchak, *Cryst. Res. Technol.* **26**, 931 (1991).

¹⁸A. S. Andrushchak, B. G. Mytsyk, and O. V. Lyubych, *Ukr. Phys. J.* **37**, 1217 (1992) (in Ukrainian).

¹⁹O. G. Vlokh, B. G. Mytsyk, A. S. Andrushchak, and Y. V. Pryriz, *Crystallogr. Rep.* **45**, 138 (2000).

²⁰A. S. Andrushchak, V. T. Adamiv, O. M. Krupych, I. Martynuk-Lototska, Y. V. Burak, and R. O. Vlokh, *Ferroelectrics* **238**, 299 (2000).

²¹A. S. Andrushchak, Y. V. Bobitski, M. V. Kaidan, B. V. Tybinka, A. V. Kityk, and W. Schranz, *Opt. Mater.* **27**, 619 (2004).

²²M. V. Kaidan, B. V. Tybinka, A. V. Zadorozhna, W. Schranz, B. Sahraoui, A. S. Andrushchak, and A. V. Kityk, *Opt. Mater.* **29**, 475 (2007).

²³N. M. Demyanyshyn, B. G. Mytsyk, A. S. Andrushchak, and O. V. Yurkevych, *Crystallogr. Rep.* **54**, 306 (2009).

²⁴A. S. Andrushchak, O. V. Yurkevych, B. G. Mytsyk, B. Sahraoui, and A. V. Kityk, *J. Appl. Phys.* **106**, 073510 (2009).

²⁵I. C. Chang, *Opt. Eng.* **24**, 132 (1985).

²⁶D. F. Nelson, *Electric, Optic and Acoustic Interaction in Dielectric* (Wiley, New York, 1979).

²⁷V. S. Bondarenko, O. A. Byshevskii, N. V. Perelomova, and L. E. Chirkov, *Sov. Phys. Crystallogr.* **30**, 127 (1985).

²⁸J. F. Nye, *Physical Properties of Crystals* (Clarendon, Oxford, 1992).

²⁹V. L. German, *Dokl. Akad. Nauk SSSR* **48**, 95 (1945) (in Russian).